PREDICTION OF THE REYNOLDS STRESSES IN TURBULENT SHEAR FLOWS WITH THE USE OF STOCHASTIC DIFFERENTIAL EQUATIONS

Daniel Irigon de Irigon, Luís Fernando Figueira da Silva, Angela Ourivio Nieckele
Department of Mechanical Engineering, Pontifícia Universidade Católica do Rio de Janeiro
Rua Marquês de São Vicente, 225; 22453-900 Rio de Janeiro, RJ Brazil
{dirigon, luisfer, nieckele}@mec.puc-rio.br

Abstract. *The objective of this study is to perform a sensitivity analysis of stochastic differentials equations for computation of the Reynolds stresses in a turbulent flow using a hybrid Eulerian/Lagrangean modelling. In this study an average shear flow is imposed, whereas the Reynolds stresses and the characteristic time scale of the turbulent fluctuations are determined through a Monte Carlo method. The Reynolds stress results were compared with available experimental data, and reasonable qualitative agreement was obtained. It was shown that the inlet turbulent frequency significantly influences the Reynolds stress distribution.*

Keywords: *turbulence, stochastic models, shear flow*

1. Introduction

Despite the rapid advancement in computational power, the direct numerical simulation of complex turbulent reactive flow fields representative of situations of practical interest remains beyond reach. This is a driving force for the development of turbulence and combustion models. This study explores the numerical features of a hybrid (Eulerian - Lagrangian) turbulence model (Muradoglu *et al.*, 1999, and Jenny *et al.*, 2001) intended to be applied to the computation of combustion. Classical turbulence models, (Kuznetsov and Sabel'nikov, 1990 and Peters, 2000) including two-equation models and second-moment closures, use Reynolds averaging techniques, yielding model equations for the statistical moments of the velocity fluctuations. In this work, these statistical moments are closed by joint velocity-frequency probability density function equations (Pope, 1985), which provide the advantage that convection is represented without modelling assumptions. In this approach, the average velocity is computed by a finite-volume method (Patankar, 1980), whereas, in contrast to moment-closure model equations, the modelled joint Probability Density Function transport equation is solved by a Lagrangian Monte-Carlo method in which particles are dispersed within the flow field Jenny *et al.* (2001). The solution of these stochastic equations provides the Reynolds stresses.

The solution procedure adopted requires the integration of stochastic differential equations in the form of Langevin equations (Gardiner, 2002), which describe the particle properties. The numerical procedure developed is validated by comparisons with experimental results of Gutmark and Wygnanski (1976), Heskestad (1965) and Bradbury (1965), in the case of a planar turbulent non reactive jet flow.

2. Description of the experimental data for validation purposes

The experimental work of Gutmark and Wygnanski (1976), is used as basis for comparison of the present computational results. In their experiment, the airflow is discharged through a rectangular orifice of width $d = 13$ mm and length $l = 500$ mm. Figure (1) gives a schematic representation of the jet flow considered. This experiment was chosen since the average flow was determined to be two-dimensional, except in the vicinity of the wall. The Reynolds number based on d was 3×10^4 and the incoming flow turbulence level was about 0.2%. However, a detailed characterization of the jet discharge is not given, thus the energy content will be assumed to be evenly distributed among the three velocity components and zero correlation coefficients will be assumed for these variables. Detailed measurements of the Reynolds stresses are provided which will be used for comparison with the present results.

In the present computations, the mean velocity is imposed, whereas fluctuating properties are computed with the stochastic Lagrangian method. This is a necessary step in the development of a fully coupled Eulerian/Lagrangian code.

The mean axial velocity field was based in measurements by Bradbury (1965), and it is given by:

$$\frac{v_0(v_0 - v_\infty)}{(\widetilde{v}_{1max} - v_\infty)^2} = 0.188\left(\frac{x}{d} - 3\right), \tag{1}$$

where x is the axial distance from the nozzle, v_0 is the velocity at the plane of the nozzle, v_∞ is the lateral velocity, as shown in Fig.(1) and $\widetilde{v}_{1max}$ is the centerline velocity of the planar jet at a given x. Note that for $x = 0$, $\widetilde{v}_{1max} = v_0$. Equation (1) degenerates into the classical decay law of a jet,

$$\widetilde{v}_{1max} \propto x^{-1/2}, \tag{2}$$

in quiescent surroundings as $v_\infty \longrightarrow 0$.

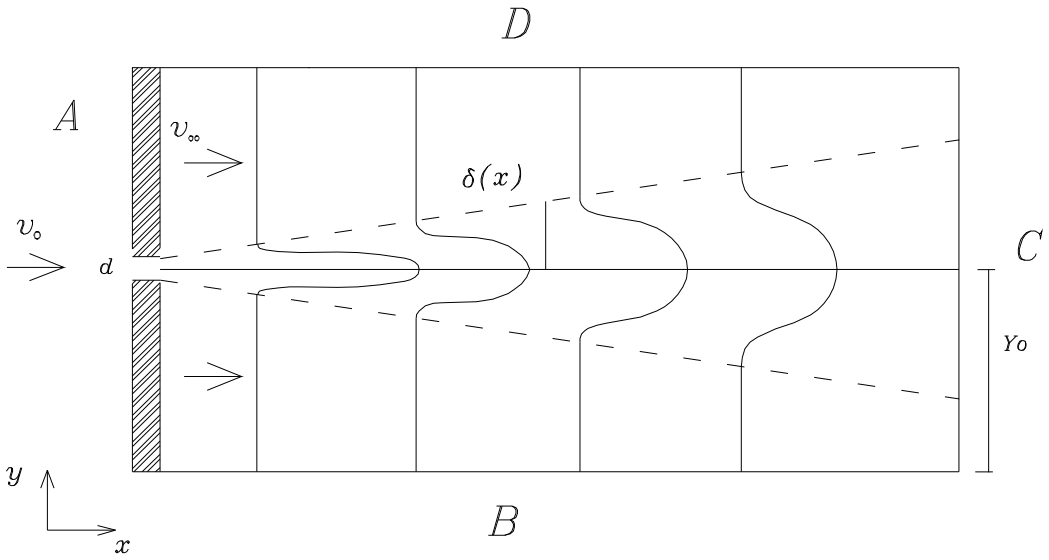

Figure 1. Schematic representation of the computational domain adopted for the planar jet modelling.

The classical form for the mean axial velocity profile is used

$$\widetilde{v}_1(\eta) = \left[\frac{1}{\cosh(\alpha\,\eta)^2}\right]\widetilde{v}_{1max}, \tag{3}$$

where α is a constant and η is the dimensionless distance from the plane of symmetry,

$$\eta = \frac{y - y_o}{\delta} \quad ; \qquad \text{with} \quad \delta = 0.1\,x + 0.2\,d, \tag{4}$$

and y_o is the distance between the centerline of the jet and the origin coordinate, as shown in Fig.(1).

The transversal velocity, v_2 is obtained applying the steady state continuity equation, $\nabla\rho\mathbf{v} = 0$.

Concerning now the measured velocity fluctuations (Gutmark and Wygnanski, 1976), Figs. (2), (3) and (4) reports the hot-wire anemometer results for the dimensionless Reynolds stresses. This figure allows to verify that the jet flow is self-similar with respect to the second moments of velocity, which further supports the self-similarity assumption used for the average velocity.

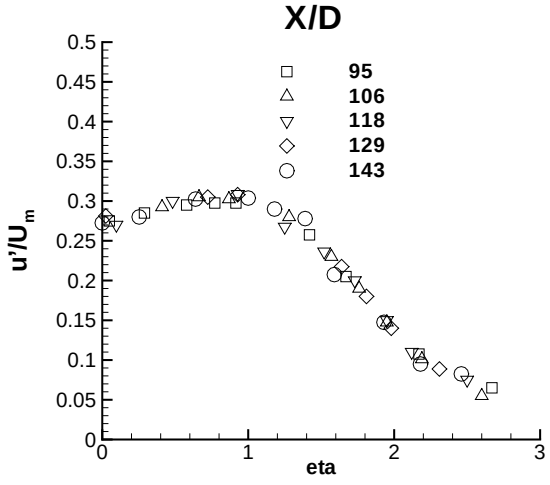

Figure 2. Experimental results of convectional distribution of the axial velocity fluctuations.

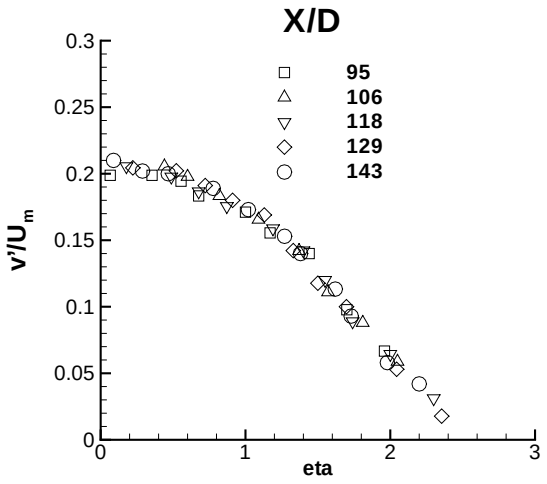

Figure 3. Experimental results of convectional distribution of the transverse velocity fluctuations.

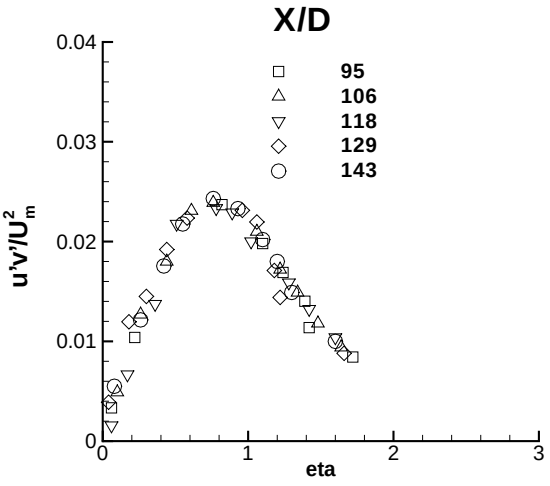

Figure 4. Experimental results of convectional distribution of the turbulent shear stress.

Note that measurements of the length or time scale of turbulent are not given by Gutmark and Wignanski (1976). Thus, an analysis will be performed in this work which allows to assess the influence of the turbulent frequency on the computed results.

3. Mathematical formulation of the problem

In this section is detailed the stochastical equation model used to describe the velocity fluctuation, particle motion and turbulent frequency.

3.1 Stochastic velocity equation

Haworth and Pope (1987), suggest that the stochastic differential equation (or Langevin equation) for velocity evolution should be:

$$dv_i^* = -\frac{1}{\overline{\rho}}\frac{\partial \overline{p}}{\partial x_i}dt + G_{ij}(v_i^* - \widetilde{v}_i)dt + B^{\frac{1}{2}}dW_i, \quad i = 1, 2, 3, \tag{5}$$

where the notation (*), is used to distinguish the modelled particle from the fluid particle, $\overline{p}$ and $\overline{\rho}$ represent respectively the Reynolds average pressure and density mass. Throughout this paper, over bars and tildes denote Reynolds and Favre averages, respectively.

This equation represents the movement of a fluid particle in the random space of variable V_i, i.e., the possible particle velocity values v_i^* that can be found around the average velocity $\widetilde{v}_i$. In this work, the average velocity is fixed from the experimentally determined values described in the previous section. Particle velocity evolves under the influence of pressure gradient, mixing with the surrounding fluid and turbulent diffusion. This latter term is stochastic in nature and analogous to a Brownian process.

In Eq. (5), G_{ij} is a second order tensor which models mixing, dW_i is a Wiener process (Gardiner, 2002) i.e., a normal distribution with null average and variance dt and B is a parameter that represent the weight of the turbulent diffusion process in the Langevin equation. Haworth and Pope (1987), model the G_{ij} tensor as a function of the Reynolds stresses, velocity gradient and turbulent kinetic energy dissipation rate, $G_{ij} = G_{ij}\left(\widetilde{u_i u_j}, \frac{\partial \widetilde{v}_i}{\partial x_j}, \varepsilon\right)$. Stochastic models with various degrees of sophistication can be obtained by analogy between Eq.5 and the Reynolds Averaged Navier-Stokes equations, (Haworth and Pope, 1986, 1987 , and Pope, 2000). In this work, the Simplified Langevin Model developed by Pope, 1983, is used,

$$G_{ij} = \frac{1}{\tau_t}\left(\frac{1}{2} + \frac{3}{4}C_0\right)\delta_{ij}, \tag{6}$$

where $C_0 = 2.1$, τ_t is the characteristic turbulence time scale and δ_{ij} is the Kronecker delta.

The characteristic time scale τ_t of the turbulent fluctuations is modelled as the inverse of the conditional turbulence frequency, (Van Slooten and Pope, 1997)

$$\Omega \equiv C_\Omega \frac{\langle \rho^* \omega^* | \omega^* \geq \widetilde{\omega} \rangle}{\overline{\rho}}. \tag{7}$$

The variables ω^* and $\widetilde{\omega}$ are the instantaneous and the average turbulence frequency of a fluid particle, the angle brackets represent the expectancy of a variable and the vertical bar denotes conditional averaging.

It is convenient to extract from the Langevin equation the average velocity, in order to obtain a stochastical equation for the velocity fluctuation v''. This may be achieved by decomposing the material derivative of v_i^* in $\widetilde{v}_i$ and $v_i''^*$,

$$\frac{dv_i}{dt} = \frac{dv_i''}{dt} + v_j''\frac{\partial \widetilde{v}_i}{\partial x_j} + \widetilde{v}_j\frac{\partial \widetilde{v}_i}{\partial x_j} + \frac{\partial \widetilde{v}_i}{\partial t}, \quad i = 1,2,3, \tag{8}$$

and by substituting in Eq.(5) one can obtain

$$dv_i''^* = \frac{1}{\bar{\rho}}\frac{\partial}{\partial x_j}\left(\bar{\rho}\widetilde{v_i'' v_j''}\right)dt - v_j''^*\frac{\partial \widetilde{v}_i}{\partial x_j}dt - \left(\frac{1}{2} + \frac{3}{4}C_0\right)\Omega v_i''^* dt + (C_0 k\Omega)^{1/2} dW_i, \quad i = 1,2,3. \tag{9}$$

Note that the mean of $v_i''^*$ in Eq.(9) is null. The Reynolds stresses may be obtained from this equation by ensemble averaging groups of Lagrangian fluid particles.

3.2 Stochastical equation for turbulent frequency

The closure of Eqs. (5) or (9), requires a model for the turbulent frequency evolution, so that the conditional frequency, Ω, may be determined by Eq.(7). In the joint pdf of velocity-frequency equation, turbulence frequency, ω^*, is a property of the particle and is model by a stochastic differential equation

$$d\omega^* = -C_3(\omega^* - \widetilde{\omega})\Omega dt - S_\omega \Omega \omega^* dt + (2C_3 C_4 \widetilde{\omega}\Omega\omega^*)^{1/2} dW. \tag{10}$$

This equation was proposed by Pope, 1994, and it has as main feature the deterministic source term S_ω similar to the well know $\kappa - \omega$ model (Wilcox, 1988). The constant $C_3 = 1.0$, was determined on the basis of Direct Numerical Simulation and $C_4 = \sigma^2 = 0.25$ (Van Slooten and Pope, 1997),

$$S_\omega = C_{\omega 2} - C_{\omega 1}\frac{P}{k\Omega}. \tag{11}$$

In this source term the constants $C_{\omega 1}$ and $C_{\omega 2}$ are 0.56 and 0.9, respectively, and P is the turbulent production term

$$P = -\widetilde{v_i v_j}\frac{\partial \widetilde{v}_i}{\partial x_j}. \tag{12}$$

In homogenous isotropic turbulence, the Probability Density Function of ω is a Gamma Distribution (Van Slooten and Pope, 1997). This distribution was found to be a fair approximation to the classical log-normal distribution, albeit with a smaller computational cost.

3.3 Particle motion

Once the average and fluctuating velocities are known, the evolution of particle in physical space is given by

$$dx_i^* = (\widetilde{v}_i + v_i'^*)dt, \tag{13}$$

where x_i^* is the instantaneous particle position.

4. Numerical method

In order to integrate the stochastic differential Eqs.(9, 10 and 13), a second-order accuracy predictor-corrector scheme was used (Haworth and Pope, 1986). The first half step applied to particle motion is:

$$x_i^{*^{n+\frac{1}{2}}} = x_i^{*^n} + \frac{\Delta t}{2}\left(\widetilde{v}_i^n + v_i'^{*^n}\right), \quad i = 1,2,3, \tag{14}$$

where the mean velocity $\widetilde{v}_i^n$ is prescribed from the experimental values, Eq.(1) at each particle position. This step is performed to obtain the midpoint particle position $x_i^{*n+1/2}$. The superscript n and $n+1$ denote the current and the new time level, respectively.

The velocity and turbulence stochastical models are integrated to the midpoint position. Defining

$$a_i = \frac{1}{\overline{\rho}}\frac{\partial}{\partial x_j}\left(\overline{\rho}\widetilde{v_i'' v_j''}\right), \qquad b_{ij} = -\frac{\partial \widetilde{v}_i}{\partial x_j} - \left(\frac{1}{2} + \frac{3}{4}C_0\right)\Omega\delta_{ij}, \qquad c = C_0\Omega k, \tag{15}$$

Eq.(9) can be written as

$$dv_i'^* = a_i dt + b_{ij}v_j'^* dt + c^{1/2}dW_i, \quad i = 1,2,3 \tag{16}$$

The coefficients, of this equation are available by ensemble averaging of stochastic particles and interpolated to a midpoint cell position.

To solve Eq.(16) the following predictor-corrector scheme (Haworth and Pope, 1986) is applied

$$\Delta v_i'^* = \left(a_i + b_{ij}v_j'^{*^n}\right)\Delta t + (c\Delta t)^{1/2}\xi_i, \quad i = 1,2,3, \tag{17}$$

$$v_i'^{*^{n+1}} = v_i'^{*^n} + \Delta v_i'^* + \frac{1}{2}b_{ij}\Delta v_j'^*\Delta t, \quad i = 1,2,3. \tag{18}$$

where ξ_i is vector of independent random variables with standard normal distribution.

The turbulence frequency model Eq.(10) can be written as

$$d\omega^* = Adt - B\omega^* dt + (C\omega^*)^{1/2}dW, \tag{19}$$

where

$$A = C_3\widetilde{\omega}\Omega, \qquad B = (C_3 + S_\omega)\Omega, \qquad C = 2C_3C_4\widetilde{\omega}\Omega. \tag{20}$$

The numerical integration of Eq.(20) proceeds by considering that the coefficients A, B and C are frozen during one time step, and evaluated at the particle midpoint position. Therefore, the expression for the mean and variance of $\omega^*(t+\Delta t)$ conditioned on $\omega^*(t) = \omega^{*^n}$ is

$$\omega^{*^{n+1}} = \max(0, \chi + \sigma\xi), \tag{21}$$

with,

$$\chi = \omega^{*^n}\exp(-B\Delta t) + \frac{A}{B}\left[1 - \exp(-B\Delta t)\right], \tag{22}$$

$$\sigma^2 = \frac{C\Delta t}{2(1+B\Delta t)}\left(\chi + \omega^{*^n}\right). \tag{23}$$

Where ξ is a random variable with standard normal distribution, independent of that of the velocity model. Note that this model guarantees realizability of the turbulent frequency, i.e., $\omega^* > 0$.

Once the velocity has been integrated, the second step is used to compute the particle position on new time level,

$$x_i^{*^{n+1}} = x_i^{*^{n+1/2}} + \Delta t\left[\widetilde{v}_i^n\left(x_i^{*^{n+1/2}}\right) + \frac{1}{2}\left(v_i'^{*^n} + v_i'^{*^{n+1}}\right)\right], \quad i = 1,2,3. \tag{24}$$

5. Boundary conditions

The set of stochastic differential equations, Eqs. (9, 10 and 13), describe the evolution of fluid particles properties in space of variables. On the Monte-Carlo method adopted, fluid particles enter the computational domain through the left, lower and upper boundaries, Fig. (1) at each time step. Note that symmetry around the x axis is not assumed, so that the code can be verified to be symmetrical *a posteriori*. Particles which leave the domain once they cross the right, lower and upper boundaries and are immediately reassigned to an inflow boundary, thus, the number of particles within the domain remains constant throughout the computation.

Care is exercised to ensure a proper particle distribution in the computational domain throughout the calculation. Particles enter the computational domain with a statistical distribution of position weighed on both the average value of velocity imposed at entrance and the thickness of the finite-volume mesh. Therefore, the cells that possess larger velocity and smaller thickness are assigned with the largest weight in the distribution, and thus receive the largest number of particles. This was found to be crucial to an adequate representation of the flow statistics.

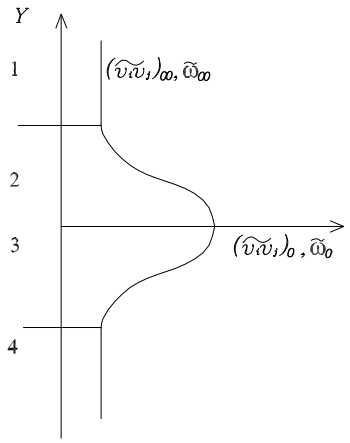

Figure 5. Distribution of the Reynolds stresses and turbulent frequency on the entrance.

Once the entrance position of a particle is know, other properties must be assigned. The velocity fluctuation at a given boundary satisfies a normal distribution with prescribed Reynolds stresses, Fig.(5), where indices 0 and ∞ refer to the variable value in the centerline and in the jet surrounding region, respectively. As suggested by Pope, 1994, the incoming particle turbulence frequency satisfies a Gamma distribution with variance $\sigma^2 = 1/4$.

6. Results and discussion

To analyze the performance of the model described, the Reynolds stresses are determined, with an imposed average shear flow. The influence of the central turbulent frequency of the jet, ω_0, as shown in Fig.(5), is investigated. Three different values are considered: 0.1; 1 and 10 s^{-1}. The frequency of the surrounding jet is maintained constant equal to 0.01 s^{-1}. For all computations the dimensionless trace of the Reynolds Stress Tensor of the central jet and surrounding region are defined as $\left(\widetilde{v_i''v_i''}\right)_0 = 36$ cm^2/s^2 and $\left(\widetilde{v_i''v_i''}\right)_\infty = 0.01$ cm^2/s^2, whereas off-diagonal terms are zero at the entrance.

The evolution of the non dimensional Reynolds stresses $\widetilde{v_i''v_i''}$ are obtained and compared with experimental results presented in Figs. (2), (3) and (4).

The present results are shown in Figs.(6), (7) and (8) and correspond, respectively, to the sets $(10; 0.01)$, $(1; 0.01)$ and $(0.1; 0.01)$ s^{-1}. The curves represent non dimensional components of Reynolds stresses at different axial positions, which normalized by the orifice diameter, i.e., $x/d = 95$, 106, 118, 129 and 143.

Note that the results are strongly influenced by the turbulent frequency boundary condition. It can be seen that the major influence is on the normal stress $\widetilde{v_1''^2}$ and, consequently, on the autocorrelation $\widetilde{v_1''v_2''}$. As expected from the experimental data, Figs. (2-4), self similar results should be predicted. Indeed, although small deviations can be seen, it can be said that the results presented self similarity. However, the numerical model was uncapable to represent the order of magnitude of the second moments of the turbulent velocities. This may be due to the adoption of an imposed average shear flow, which did not allow the evolution of the averaged velodities to adjust during the solution process. Another observation is that the integration of stochastic equation for turbulent frequency is a function of production term and presents an exponential time dependence, Eqs. (20, 22), therefore, for high velocities gradients, special care must be taken, because

the exponent of Eq. (22) can grow rapidly, and therefore small time steps should be used.

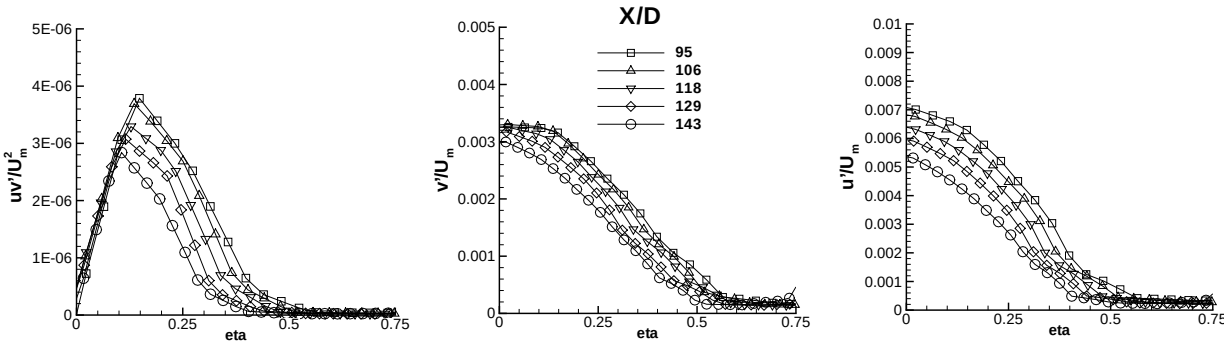

Figure 6. Non dimensional transversal evolution of shear stress, lateral velocity fluctuation and axial velocity fluctuation, for values of turbulent frequency on the centerline of the jet and surround, respectively $\omega_0 = 10s^{-1}$ and $\omega_\infty = 0.01s^{-1}$.

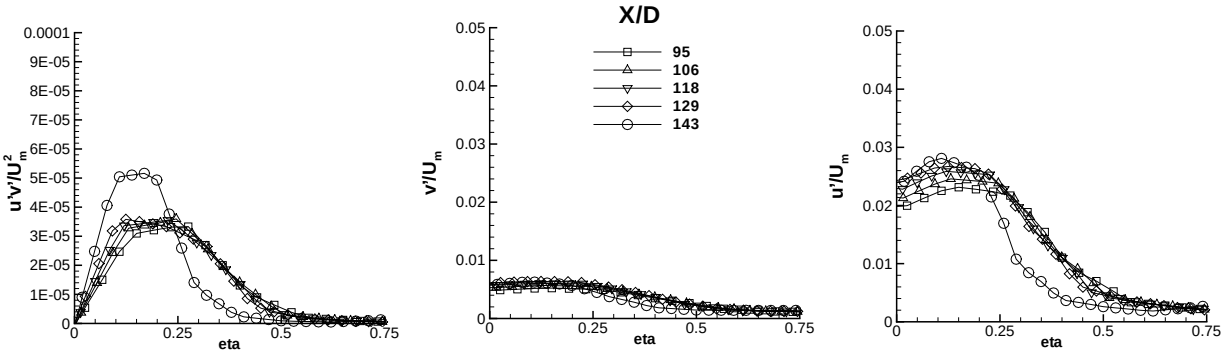

Figure 7. Non dimensional transversal evolution of shear stress, lateral velocity fluctuation and axial velocity fluctuation, for values of turbulent frequency on the centerline of the jet and surround, respectively $\omega_0 = 1s^{-1}$ and $\omega_\infty = 0.01s^{-1}$.

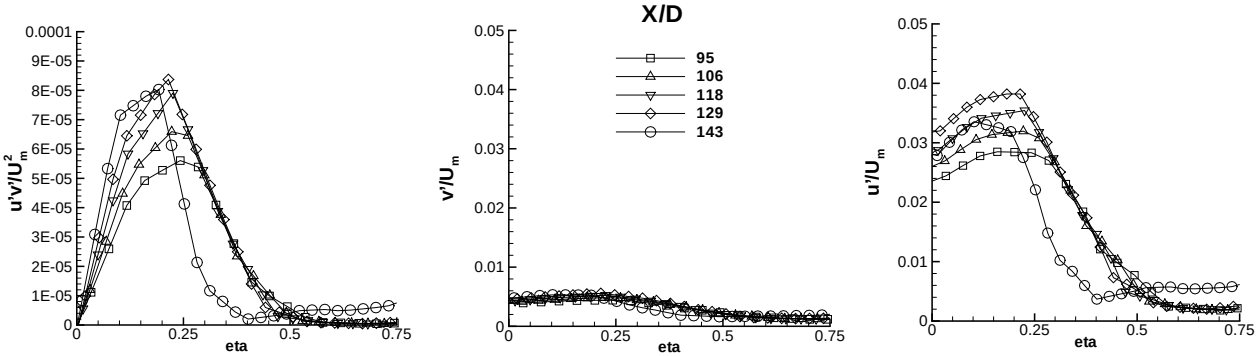

Figure 8. Non dimensional transversal evolution of shear stress, lateral velocity fluctuation and axial velocity fluctuation, for values of turbulent frequency on the centerline of the jet and surround, respectively $\omega_0 = 0.1s^{-1}$ and $\omega_\infty = 0.01s^{-1}$.

7. Conclusion

This work presented an analysis of the stochastic differentials equations for computation of the Reynolds stresses for a planar free jet, with an imposed average shear flow. This is the first step to develop a hybrid Eulerian/Lagrangean model. The results obtained are promising, leading to the next step which is the coupling of the determination of the Reynolds stresses through a Monte Carlo method with the average flow, to be determined by a finite volume method.

8. Acknowledgements

The authors thank CNPq and CAPES for the support during the development of this work. During this work L. F. Figueira da Silva was on leave from *Laboratoire de Combustion et de Détonique, Centre Nacional de la Recherche Scientifique*, France, with a PROFIX scholarship from CNPq-Brazil.

9. References

Bradbury, L.J.S., 1965, "The Structure of a Self-Preserving Turbulent Plane Jet", Journal of Fluid Mechanics, Vol. 23, pp. 31-64.

Dopazo, C., 1994, "Recent Developments in PDF Methods", Edited by Libby P.A and F.A Williams, London, 375 p.

Gardiner, C.W., 2002, "Handbook of Stochastic Methods", 6th edition, New York, 444 p.

Gutmark, E., Wygnanski, I., 1976, "The Planar Turbulent Jet", Journal of Fluid Mechanics, Vol. 73, pp. 465-495.

Haworth, D.C., Pope, S.B., 1986, "A Generalized Langevin Model for Turbulent Flows", Physics of Fluids, Vol. 29, pp. 387-405.

Haworth, D.C., Pope, S.B., 1987, "A PDF Modeling Study of Self-Similar Turbulent Free Shear Flows", Physics of Fluids, Vol. 30, pp. 1026-1044.

Heskestad, G., 1965, "Hot-Wire Mensurements in a Plane Turbulent Jet", Journal of Applied Mechanics, Vol. 32, pp. 721-734.

Jenny, P., Pope, S.B., Muradoglu, M., Caughey, D.A., 2001, "A Hybrid Alghorithm for the Joint PDF Equation of Turbulent Reactive Flows", Journal of Computational Physics, Vol. 166, pp. 218-252.

Kuznetsov, V.R. Sabel'nikov, V.A., 1990, "Turbulence and Combustion", Hemisphere Publishing Corporation, New York, USA.

Muradoglu, M., Pope, S.B., Jenny, P., Caughey, D.A., 1999, "A Consistent Hybrid Finite-Volume/Particle Method for the PDF Equation of Turbulent Reactive Flows", Journal of Computational Physics, Vol. 154, pp. 342-371.

Patankar S.V., 1980, "Numerical Heat Transfer and Fluid Flow", Hemisphere Publishing Corporation, New York, USA, 195 p.

Peters N., 2000, "Turbulent Combustion", Cambridge University Press, Cambridge, UK.

Pope, S.B., 1983, "A Langevin Two-Time Probability Density Function Equation for Inhomogeneous Turbulent Flows", Physics of Fluids, Vol. 26, pp. 3348-3450.

Pope, S.B., 1985, "PDF Methods for Turbulent Reactive Flows", Progress in Energy and Combustion Science, Vol. 11, pp. 119-192.

Pope, S.B., 1985, "A Generalized Langevin Model for Turbulent Flows", Physics of Fluids, Vol. 29, pp. 387-405.

Pope, S.B., 1994, "Lagrangian PDF Methods for Turbulent Flows", Annual Review of Fluid Mechanics, Vol. 26, pp. 23-63.

Pope, S.B., 2000, "Turbulent Flows", Cambridge University Press, Cambridge, United Kingdom, 771 p.

Van Slooten, P.R., Pope, S.B. 1997, "PDF Modeling of Inhomogeneous Turbulence with Exact Representation of Rapid Distortions", Physics of Fluids, Vol. 9, pp. 1085-1105.

Wilcox D.C. 1988, "Multiscale Model for Turbulent Flows", American Institute of Aeronautics and Astronautics, Vol. 26, pp. 1311-1320.